HNPS Advances in Nuclear Physics

Vol 27 (2019)

HNPS2019

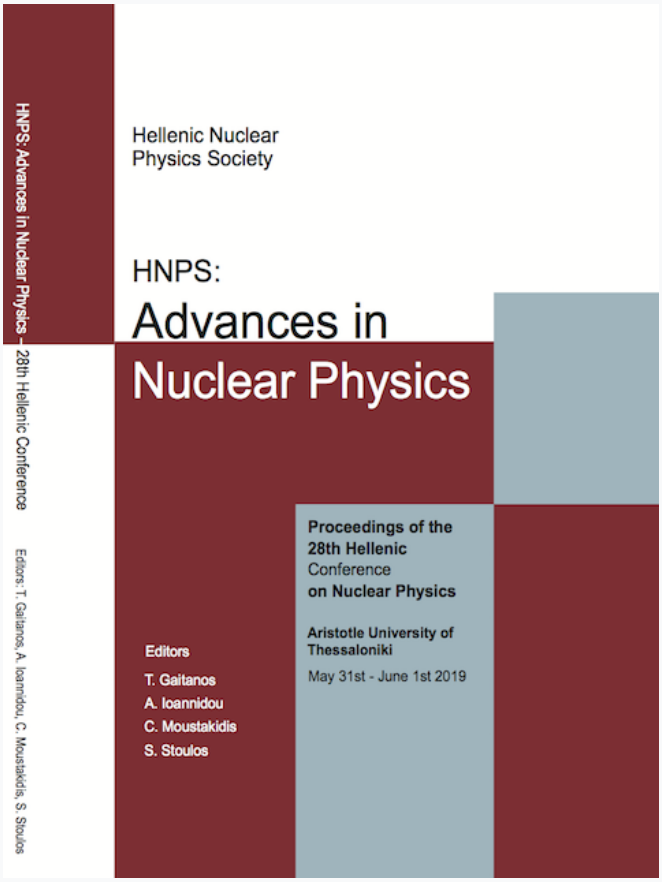

An Investigation on Gamma-Ray Shielding Properties of Zr-Based Bulk Metallic Glasses

M. Şekerci, H. Özdoğan, A. Kaplan

doi: 10.12681/hnps.2477

HNPS Advances in Nuclear Physics vol. 27, pp. 48–55 (2020)
HNPS2019
doi:10.12681/hnps.2477

An Investigation on Gamma-Ray Shielding Properties of Zr-Based Bulk Metallic Glasses

M. Şekerci[1], H. Özdoğan[2], A. Kaplan[1]

[1] *Süleyman Demirel University, Department of Physics, 32260, Isparta, Turkey*
[2] *Akdeniz University, Department of Biophysics, 07070, Antalya, Turkey*

Abstract *Studies on bulk metallic glasses (BMGs) have grown considerably, especially in recent years, due to their noticeable properties such as high glass forming ability, corrosion resistance, large elastic limit, chemical, mechanical and magnetic properties. Among the known and studied samples of BMGs, Zr-based ones have been appointed as possible examples in biomaterial and structural material studies due to their good mechanical and corrosive properties and good biocompatibility. In this study, considering the importance of Zr-based BMGs, an investigation on their gamma-ray shielding properties have been done where five different samples have been utilized which are* $Zr_{51}Al_{14.2}Ni_{15.9}Cu_{18.9}$, $Zr_{52}Al_{12.9}Ni_{13.8}Cu_{21.3}$, $Zr_{53}Al_{11.6}Ni_{11.7}Cu_{23.7}$, $Zr_{54}Al_{10.2}Ni_{9.4}Cu_{26.4}$ *and* $Zr_{55}Al_{8.9}Ni_{7.3}Cu_{28.8}$. *Mass attenuation coefficients of the samples have been obtained by using Geant4 and XCOM between 0.1-15 MeV incident photon energy. Also, mean free path (MFP), half-value layer (HVL), tenth-value layer (TVL), effective atomic number (*Z_{eff}*) and electron density (*N_{eff}*) values of the samples in the given energy range have been obtained. Obtained results have been graphed for better visual comparison and interpretation*

Keywords *Zr-based BMG, XCOM, Geant4, mass attenuation coefficient*

Corresponding author: M. Şekerci (mertsekerci@sdu.edu.tr) | *Published online*: May 1st, 2020

INTRODUCTION

Bulk metallic glasses (BMG), which are also known as amorphous metals, have been studying since their first production around 1960 [1]. Since then, many studies have been performed on their physical and chemical characteristics as well as on their production improvements [2-6]. In contrast to the conventional metals, in where the atoms are arranged in a repeating pattern of crystals or grains with different sizes and shapes, BMGs do not have repeating patterns and their atomic structure have been formed within a random and disordered structure. This amorphous structure, which is lack of grain defects, provide BMG's competitive superior physical characteristics such as strength, toughness, hardness, elasticity, corrosion and wear resistance. Many different metal based forms of them, such as Zr [7], Al [8], Ti [9], Fe [10], Co [11], Mg [12] and etc. have been generated and studied in the manners of production and physical/chemical properties. In addition to these studies, investigations on the radiation shielding properties of BMGs can be performed by taking into account of their wide usage and application areas that they have and may have. With this motivation, gamma-ray shielding properties of five Zr–based BMG samples were investigated in this study where the samples were selected as $Zr_{51}Al_{14.2}Ni_{15.9}Cu_{18.9}$, $Zr_{52}Al_{12.9}Ni_{13.8}Cu_{21.3}$, $Zr_{53}Al_{11.6}Ni_{11.7}Cu_{23.7}$, $Zr_{54}Al_{10.2}Ni_{9.4}Cu_{26.4}$ and $Zr_{55}Al_{8.9}Ni_{7.3}Cu_{28.8}$. For the investigated samples mass attenuation coefficient values were obtained by using both XCOM [13] and GEANT4 [14]. Later on, mean free path (MFP), half value layer (HVL), tenth value layer (TVL), effective atomic number (Z_{eff}) and electron density (N_{eff}) values were calculated.

THEORETICAL CALCULATIONS

In order to reach the goals of the study, firstly the density values of selected Zr–based BMGs were calculated by using molar–volume weighted average density approximation method [15] where the results are given in Table 1.

Table 1. *Density values of selected Zr-based BMGs*

Sample BMG	Density (g/cm^3)
$Zr_{51}Al_{14.2}Ni_{15.9}Cu_{18.9}$	6.5516
$Zr_{52}Al_{12.9}Ni_{13.8}Cu_{21.3}$	6.6044
$Zr_{53}Al_{11.6}Ni_{11.7}Cu_{23.7}$	6.6569
$Zr_{54}Al_{10.2}Ni_{9.4}Cu_{26.4}$	6.7143
$Zr_{55}Al_{8.9}Ni_{7.3}Cu_{28.8}$	6.7659

By using density, ρ, and the linear attenuation coefficient, μ, it is possible to obtain mass attenuation coefficient, μ_m. Linear attenuation coefficient could be defined as the fraction of attenuated incident photons in a monoenergetic beam per unit thickness of a material and has a unit of inverse-length, cm^{-1}. It could be expresses more clearly with the Beer–Lambert law which is given in Equation 1

$$I = I_0 e^{-\mu x} \tag{1}$$

where I_0 represents the original intensity of the beam, I is the beam intensity at a distance x in the material and e is the Euler's number [16]. The mass attenuation coefficient is the ratio of linear attenuation coefficient to density and generally represented with the unit of cm^{2}g^{-1}. For a compound or mixture, the mass attenuation coefficient is defined as given in Equation 2,

$$\mu_m = \frac{\mu}{\rho} = \sum w_i \left(\frac{\mu}{\rho}\right)_i \tag{2}$$

where w_i and $(\mu/\rho)_i$ are the weight fraction and the mass attenuation coefficient of the i^{th} element in the material itself, respectively [17, 18]. In this study, mass attenuation coefficients obtained by XCOM and GEANT4 softwares are calculated using this approach. Other values examined in the study can be derived from the above mentioned quantities. The mean free path could be described as the mean distance that a photon can travel between two successive interactions with the material and it is obtained by using the Equation 3

$$MFP = \frac{1}{\mu} \tag{3}$$

The thickness of the material where the transmitted radiation intensity is one-half of the incident radiation intensity is known as the half value layer while it is named as tenth value layer if the beam intensity is to 10% of its initial value. HVL and TVL can be calculated by the Equations 4 and 5, respectively.

$$HVL = \frac{ln2}{\mu} \tag{4}$$

$$TVL = \frac{ln10}{\mu} \tag{5}$$

Other two parameters obtained in this study are Z_{eff} and N_{eff} which are important parameters for better realization of a materials characteristics for various applications such as radiation shielding, dose absorbtion and etc. Z_{eff}, which is a dimensionless quantity, can be obtained as shown in Equation 6

$$Z_{eff} = \frac{\sigma_a}{\sigma_e} \tag{6}$$

where σ_a is the total atomic cross-section, in the units of cm^2/atom, and σ_e is the total electronic cross-section, in the units of cm^2/electron. Equations 7 and 8 are given to represent how σ_a and σ_e are obtained.

$$\sigma_a = \frac{\mu_m}{N_A \sum_i \frac{w_i}{A_i}} \tag{7}$$

$$\sigma_e = \frac{1}{N} \sum_i \left(\frac{\mu}{\rho}\right)_i \frac{f_i A_i}{Z_i} \tag{8}$$

In Equation 7, N_A is the Avogadro number while w_i and A_i are the weight fraction and atomic weight of the i^{th} element in the material, respectively. f_i and Z_i from the Equation 8 are used to define the fractional abundance and the atomic number of the i^{th} element in the material, respectively. By using Z_{eff}, it is possible to obtain N_{eff} in the units of electron/g as given in Equation 9.

$$N_{eff} = N \frac{Z_{eff}}{\sum_i f_i A_i} \tag{9}$$

RESULTS AND DISCUSSION

Theoretical calculations of mass attenuation coefficients from XCOM and GEANT4 were obtained for the energy range of 0.1–15 MeV. Figure 1 shows their graphical representations while Table 1 gives the obtained data and their deviation in percent.

As expected, from both XCOM and GEANT4 results the mass attenuation coefficient values decrease with the increase of energy as seen in Figure 1. On the other hand, it is easily seen from Table 1 that how the composition of the materials affect the mass attenuation coefficients. From there, it can be realized that higher mass attenuation coefficient values were obtained with the increment of Zr rate in the material and the maximum values among the studied samples were obtained from $Zr_{55}Al_{8.9}Ni_{7.3}Cu_{28.8}$.

Obtained *MFP* values of the samples were given in Figure 2. As can be seen from the figure, the *MFP* value of every sample was increased with the increase of energy and the difference between the samples are so small that almost neglectable up to almost 6 MeV. However, after that energy, the difference between the results have become more clear and they exhibited a slight decrease rather than a continuous to increase.

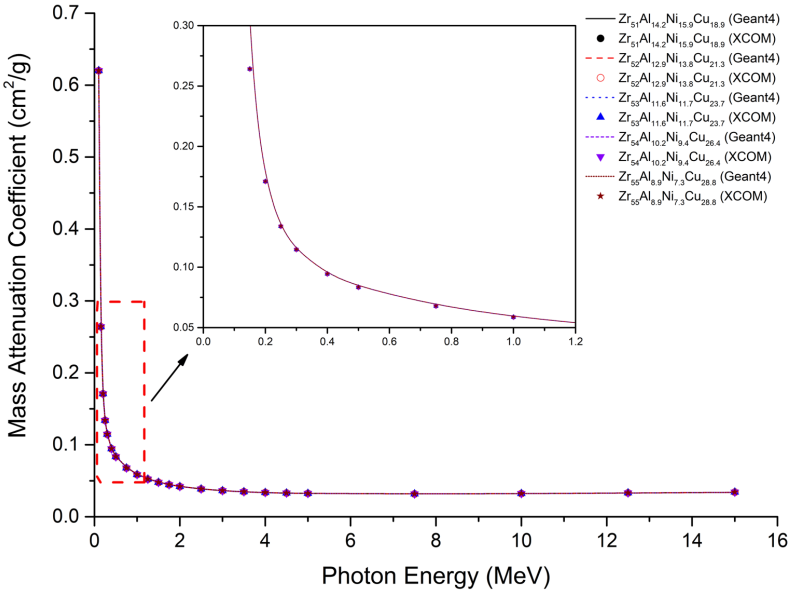

Figure 1. *Graphical representation of mass attenuation coefficient calculations*

Table 1. *Comparison of mass attenuation coefficient values*

Energy (MeV)	$Zr_{51}Al_{14.2}Ni_{15.9}Cu_{18.9}$			$Zr_{52}Al_{12.9}Ni_{13.8}Cu_{21.3}$			$Zr_{53}Al_{11.6}Ni_{11.7}Cu_{23.7}$			$Zr_{54}Al_{10.2}Ni_{9.4}Cu_{26.4}$			$Zr_{55}Al_{8.9}Ni_{7.3}Cu_{28.8}$		
	Geant4	XCOM	% Dev.	Geant4	XCOM	% Dev.	Geant4	XCOM	% Dev.	Geant4	XCOM	% Dev.	Geant4	XCOM	% Dev.
0.1	0.61696	0.6202	0.52241	0.62535	0.6286	0.51702	0.63374	0.637	0.51177	0.64241	0.6457	0.50952	0.65079	0.6542	0.52125
0.15	0.26297	0.2641	0.42787	0.26532	0.2664	0.40541	0.26768	0.2688	0.41667	0.2701	0.2712	0.4056	0.27245	0.2736	0.42032
0.2	0.17005	0.171	0.55556	0.17092	0.1719	0.5701	0.1718	0.1728	0.5787	0.17269	0.1737	0.58146	0.17356	0.1745	0.53868
0.25	0.13311	0.1339	0.58999	0.13347	0.1342	0.54396	0.13382	0.1346	0.57949	0.13418	0.1349	0.53373	0.13454	0.1353	0.56171
0.3	0.11415	0.1146	0.39267	0.11428	0.1147	0.36617	0.11441	0.1149	0.42646	0.11454	0.115	0.4	0.11468	0.1151	0.3649
0.4	0.09457	0.09446	0.11645	0.094539	0.09443	0.11543	0.094507	0.0944	0.11335	0.094467	0.09436	0.1134	0.094435	0.09433	0.11131
0.5	0.083814	0.0834	0.4964	0.083732	0.08332	0.49448	0.083651	0.08324	0.49375	0.08356	0.08315	0.49308	0.083478	0.08306	0.50325
0.75	0.068426	0.06781	0.90842	0.068319	0.0677	0.91433	0.068213	0.06759	0.92173	0.068098	0.06748	0.91583	0.067992	0.06737	0.92326
1	0.05917	0.05865	0.88662	0.059068	0.05855	0.88471	0.058965	0.05845	0.88109	0.058854	0.05833	0.89834	0.058752	0.05823	0.89645
1.25	0.052737	0.05233	0.77776	0.052643	0.05223	0.79073	0.052548	0.05214	0.78251	0.052447	0.05203	0.80146	0.052352	0.05194	0.79322
1.5	0.04814	0.04784	0.62709	0.048057	0.04776	0.62186	0.047974	0.04767	0.63772	0.047884	0.04758	0.63892	0.047801	0.04749	0.65487
1.75	0.044745	0.04454	0.46026	0.044674	0.04447	0.45874	0.044603	0.04439	0.47984	0.044527	0.04431	0.48973	0.044456	0.04424	0.48825
2	0.042166	0.04205	0.27586	0.042107	0.04198	0.30253	0.042047	0.04192	0.30296	0.041983	0.04186	0.29384	0.041924	0.04179	0.32065
2.5	0.038564	0.03856	0.01037	0.038527	0.03852	0.01817	0.03849	0.03848	0.02599	0.038449	0.03844	0.02341	0.038412	0.0384	0.03125
3	0.036242	0.0363	0.15978	0.036225	0.03628	0.1516	0.036207	0.03626	0.14617	0.036187	0.03624	0.14625	0.036169	0.03622	0.14081
3.5	0.034686	0.03477	0.24159	0.034686	0.03477	0.24159	0.034686	0.03477	0.24159	0.034684	0.03476	0.21864	0.034684	0.03476	0.21864
4	0.033621	0.03372	0.29359	0.033637	0.03373	0.27572	0.033652	0.03375	0.29037	0.033667	0.03376	0.27547	0.033682	0.03377	0.26059
4.5	0.032887	0.03299	0.31222	0.032917	0.03302	0.31193	0.032946	0.03305	0.31467	0.032976	0.03308	0.31439	0.033005	0.0331	0.28701
5	0.032385	0.03249	0.32318	0.032427	0.03253	0.31663	0.032469	0.03257	0.3101	0.032512	0.03261	0.30052	0.032554	0.03266	0.32456
7.5	0.031666	0.03179	0.39006	0.031759	0.03188	0.37955	0.031851	0.03197	0.37222	0.031947	0.03207	0.38354	0.032039	0.03216	0.37624
10	0.032151	0.03234	0.58442	0.032279	0.03247	0.58824	0.032407	0.0326	0.59202	0.032542	0.03273	0.5744	0.03267	0.03286	0.57821
12.5	0.032983	0.03323	0.7433	0.033139	0.03339	0.75172	0.033295	0.03355	0.76006	0.033458	0.03371	0.74755	0.033614	0.03387	0.75583
15	0.033907	0.03419	0.82773	0.034085	0.03437	0.82921	0.034264	0.03455	0.82779	0.034451	0.03474	0.83189	0.034629	0.03493	0.86172

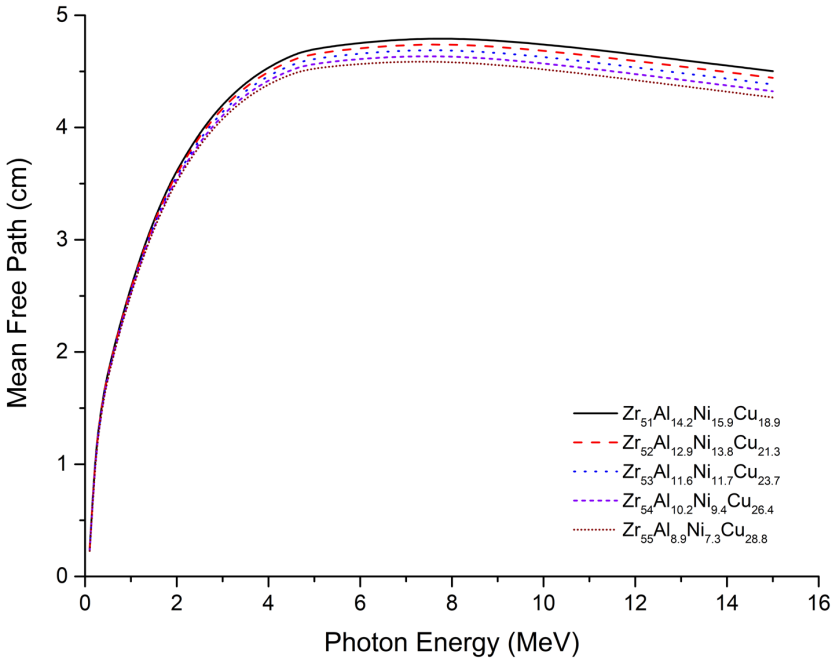

Figure 2. *MFP values of the samples*

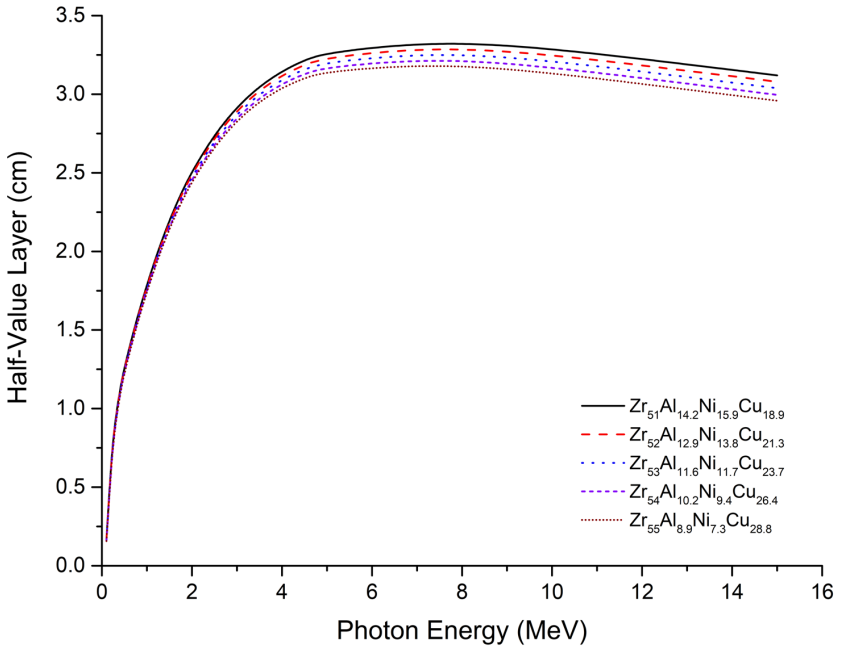

Figure 3. *HVL values of the samples*

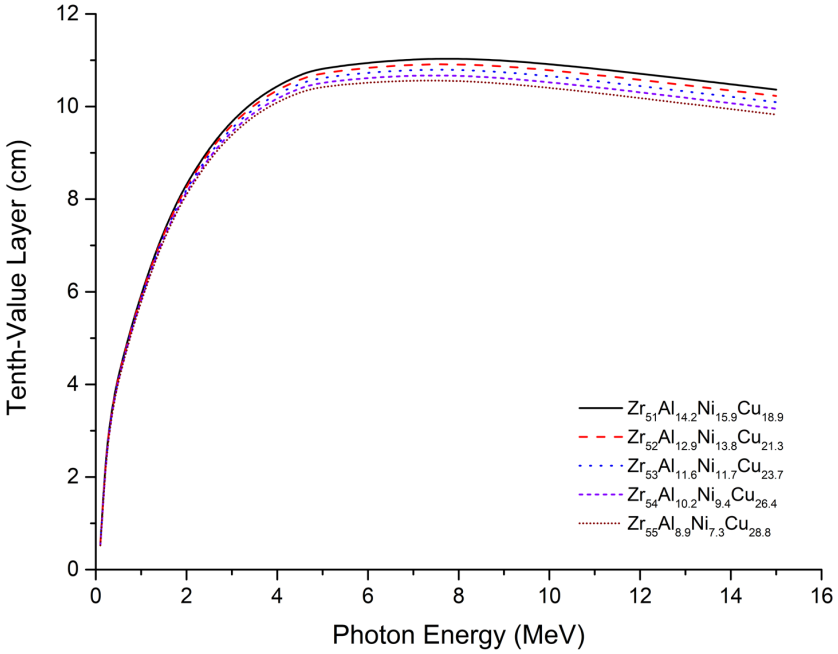

Figure 4. *TVL values of the samples*

Comparisons of the calculated *HVL* and *TVL* values for the samples were given in Figs. 3 and 4, respectively. In both figures, *HVL* and *TVL* values display an increment up to almost 4 MeV as the energy increases yet the difference between the values for the samples are not significantly remarkable up to almost 3 MeV. $Zr_{51}Al_{14.2}Ni_{15.9}Cu_{18.9}$ sample has the highest *HVL* and *TVL* values while $Zr_{55}Al_{14.2}Ni_{15.9}Cu_{18.9}$ has the lowest. Other samples represent a reduction with the increase of the Zr rate in the samples.

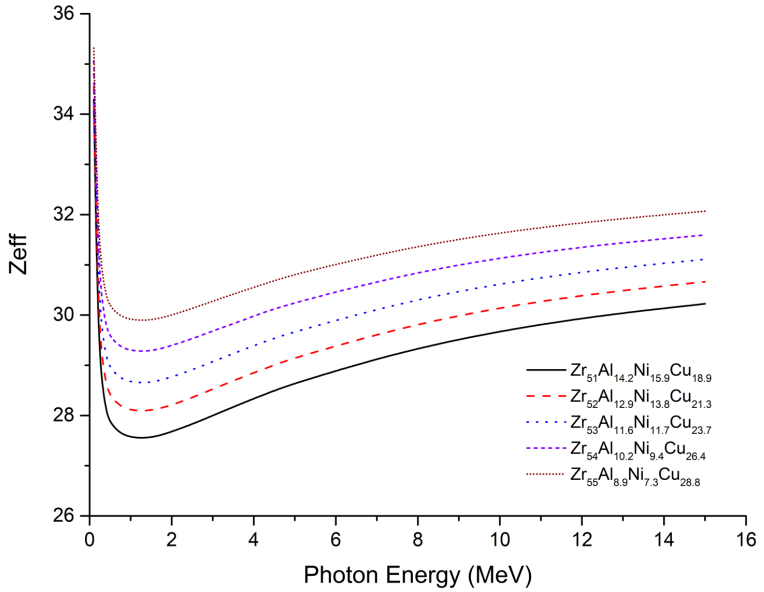

Figure 5. *Z_{eff} values of the samples*

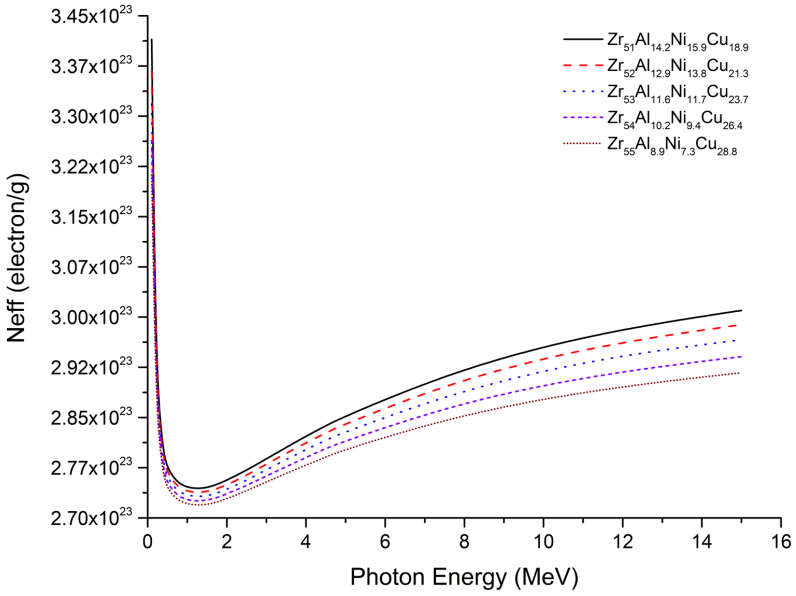

Fig. 6. N_{eff} values of the samples

The last two of all figures, which are Fig. 5 and Fig. 6, were dedicated to represent the Z_{eff} and N_{eff} calculations comparisons. In both figures, it can be seen that the calculated values increase with the increase of energy except the rapid decrease in the 0.1–1 MeV energy range. By considering the relation between the Z_{eff} and N_{eff}, the order of the samples within the graphs can be explained where the lower Z_{eff} and higher N_{eff} values were obtained with the increase of the Zr amont in the sample.

CONCLUSIONS

This study covers the theoretical calculations which are performed to obtain mass attenuation coefficient as well as MFP, HVL, TVL, Z_{eff} and N_{eff} values for five samples of Zr-based BMGs. Obtained results showed that, both computation tools, which are XCOM and GEANT4, generate quite compatible mass attenuation coefficient results with each other. The lowest and highest mass attenuation coefficient values have been calculated for the $Zr_{51}Al_{14.2}Ni_{15.9}Cu_{18.9}$ and $Zr_{55}Al_{8.9}Ni_{7.3}Cu_{28.8}$ samples, respectively. Obtained results could be compared with the experimental data in the future studies not only to provide an improvement to the computation codes but also to investigate the shielding properties of the studied samples. Also, other obtained values may contribute to the literature and may be beneficial for further studies which focus on these materials in the manner of their production, development and improvement for many industrial and scientific application possibilities.

References

[1] W. Klement, et al., Nature 187, p. 869 (1960).
[2] W.H.Wang, et al., Mater. Sci. Eng. R. Rep. 44, p. 45 (2004).
[3] M. M. Khan, et al., Crit. Rev. Solid State 43, p. 233 (2018).
[4] C. J. Byrne, et al., Science 321, p. 502 (2008).

[5] M. Jafary-Zadeh, et al., J. Funct. Biomater. 9, p. 19 (2018).
[6] D. C. Hofmann, J. Mater. 2013, p. 517904 (2018).
[7] A. Cai, et al., Materials 9, p. 408 (2016).
[8] H.C.Manjunatha, et al., Appl. Radiat. Isot. 139, p. 187 (2018).
[9] C. Ma, et al., Mater. Trans. 45, p. 3233 (2004).
[10] J. C. Khong, et al., Sci. Rep. 6, p. 36998 (2016).
[11] Z. Zhou, et al., Mater. Sci. Eng. C. Mater. Biol. Appl. 69, p. 46 (2016).
[12] H. Li, et al., Mater. Sci. Eng. C. Mater. Biol. Appl. 68, p. 632 (2016).
[13] M. J. Berger, et al., (Online) Available: http://physics.nist.gov/xcom (2019, May 13).
[14] S. Agostinelli, et al., Nucl. Instrum. Methods Phys. Res. A. 506, p. 250 (2003).
[15] B. Lohwongwatana, Thesis (Ph.D.), California Institute of Technology, (2007).
[16] J. D. J Ingle and S. R. Crouch, Spectrochemical Analysis. New Jersey: Prentice Hall, (1988).
[17] D. F. Jackson, et al., Phys. Rep. 70, p. 169-233 (1981).
[18] J.H. Hubbell, et al., S.M. Nat. Inst. Stand. Phys. Lab. (1995).